JACS
JOURNAL OF THE AMERICAN CHEMICAL SOCIETY

Article

pubs.acs.org/JACS

Evidence To Challenge the Universality of the Horiuti–Polanyi Mechanism for Hydrogenation in Heterogeneous Catalysis: Origin and Trend of the Preference of a Non-Horiuti–Polanyi Mechanism

Bo Yang,[†] Xue-Qing Gong,[†] Hai-Feng Wang,[†] Xiao-Ming Cao,*[,†] John J. Rooney,[‡] and P. Hu*[,†,‡]

[†]State Key Laboratory of Chemical Engineering, Center for Computational Chemistry and Research Institute of Industrial Catalysis, East China University of Science & Technology, Shanghai 200237, P.R. China

[‡]School of Chemistry and Chemical Engineering, The Queen's University of Belfast, Belfast BT9 5AG, U.K.

Supporting Information

ABSTRACT: The Horiuti–Polanyi mechanism has been considered to be universal for explaining the mechanisms of hydrogenation reactions in heterogeneous catalysis for several decades. In this work, we examine this mechanism for the hydrogenation of acrolein, the simplest α,β-unsaturated aldehyde, in gold-based systems as well as some other metals using extensive first-principles calculations. It is found that a non-Horiuti–Polanyi mechanism is favored in some cases. Furthermore, the physical origin and trend of this mechanism are revealed and discussed regarding the geometrical and electronic effects, which will have a significant influence on current understandings on heterogeneous catalytic hydrogenation reactions and the future catalyst design for these reactions.

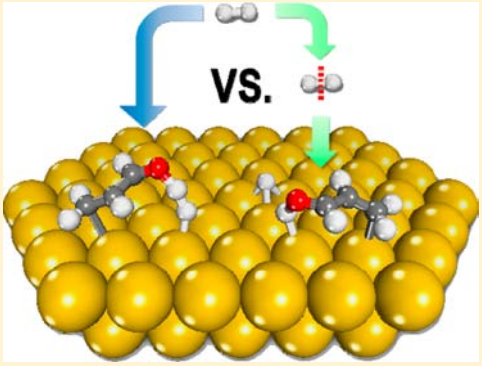

1. INTRODUCTION

To understand the mechanisms of catalytic reactions is of fundamental importance not only scientifically but also technologically: Rational design of new catalysts must rely on the insight into the reaction system provided by mechanistic studies. Among many catalytic processes, hydrogenation is one of the most important types of reactions in chemistry and widely used in almost every industrial area, such as productions of petrochemicals, fine-chemicals, and pharmaceuticals.[1−3] In particular, the selective hydrogenation of α,β-unsaturated aldehydes and ketones in heterogeneous catalysis is of intensive interest to industries for the formation of unsaturated alcohols.[1,4−8] It is also of scientific importance because of the challenging issue of selectivity in the hydrogenation of conjugated C=C and C=O functional groups. The Horiuti–Polanyi mechanism, which describes hydrogen molecule dissociation followed by the sequential addition of atomic hydrogen to the substrate, is almost universally recognized as the explanation for hydrogenation reactions since it was first proposed in the 1930s.[9−12] However, there has been tangible evidence that a sizable barrier to H_2 dissociation on some catalysts may exist and that the dissociation mechanism of H_2 may also be varied in the presence of oxygen.[13] In this work, we systematically investigate the reaction mechanisms of the selective hydrogenation of α,β-unsaturated aldehydes on a variety of Au catalysts, as well as some non-Au catalysts, using first-principles calculations. We find that a non-Horiuti–Polanyi mechanism, in which molecular hydrogen directly reacts with the substrate, is favored in some cases. The reason for the existence of the non-Horiuti–Polanyi mechanism is analyzed in detail, and some general trends are obtained. This work may have a significant impact on the design of new catalysts for hydrogenation reactions.

Like many other hydrogenation reactions, extensive studies of the hydrogenation of α,β-unsaturated aldehydes and ketones have suggested that it follows the so-called Horiuti–Polanyi mechanism. Indeed, on many transition metals, H_2 dissociation has been found to be nearly barrierless, such as hydrogenation on Pd discovered by Horiuti and Polanyi; therefore, this process is by no means the obstacle for the complete hydrogenation reaction. Yet it would still be interesting to know whether the Horiuti–Polanyi mechanism works, given that some catalysts are too inert to break the H–H bond but they are able to catalyze a variety of hydrogenation reactions, with some experimental and theoretical studies revealing the possibility of the existence of high H_2 dissociation barriers.[14,15] For example, on the surfaces of relatively inert group 11 (IB) metals, i.e., Cu, Ag, and Au, the dissociation of H_2 usually shows high barriers. Our previous density functional theory (DFT) calculations also found that on a supported Au/TiO_2 catalyst, hydrogen dissociation may occur with a free energy barrier as high as 0.95 eV. It was also reported that this process is endothermic (0.16 eV) on the Cu(111) surface with a high barrier of 0.83 eV. Considering that both Au and Cu are good catalysts for a wide range of hydrogenation reactions, one may

Received: August 10, 2013
Published: September 13, 2013

dx.doi.org/10.1021/ja408314k | J. Am. Chem. Soc. 2013, 135, 15244−15250

ask the following fundamental questions: (i) Is the Horiuti−Polanyi mechanism the universal mechanism for all hydrogenation reactions? (ii) If not, can an alternative non-Horiuti−Polanyi mechanism in which the hydrogenation occurs via the direct reaction of substrates with molecular hydrogen be found, and how does it proceed? (iii) Are there any general trends regarding the preference for Horiuti−Polanyi or non-Horiuti−Polanyi mechanism?

In order to answer these questions, in this work, we have calculated the hydrogenation of acrolein (C_3H_4O) systematically on a variety of Au catalysts as an example to address the hydrogenation mechanism using the DFT method. The system was chosen for the following reasons: First, the hydrogenation of α,β-unsaturated aldehydes (ketones) is of particular interest in a variety of industries.[1,16−18] Second, Au catalysts are very promising for the selective hydrogenation of α,β-unsaturated aldehydes and ketones since they can give rise to the highest selectivity toward the desired product, i.e., unsaturated alcohols. Third, as the simplest α,β-unsaturated aldehyde, acrolein is a good model molecule for fundamental studies.

In the current work, both Horiuti−Polanyi and non-Horiuti−Polanyi pathways are thoroughly examined over a range of catalyst surfaces (e.g., Au, Ag, and Cu) with different surface structures and coordination numbers of surface reactive atoms. In the Horiuti−Polanyi hydrogenation pathway, the reaction undergoes two elementary steps in which molecular hydrogen first dissociates on the surface, followed by subsequent hydrogenation of the substrate by the atomic hydrogen. In the non-Horiuti−Polanyi hydrogenation pathway, molecular hydrogen directly reacts with the substrate. The possible pathways of acrolein hydrogenation on the terminal carbon and oxygen atoms in acrolein are both considered in this work (Scheme 1). The origin and trend of Horiuti−Polanyi and non-Horiuti−Polanyi mechanisms are also investigated and discussed.

Scheme 1. Schematic Diagram of Hydrogenation Reactions by Both Atomic and Molecular Hydrogen on the Terminal Oxygen and Carbon in the Acrolein Molecule[a]

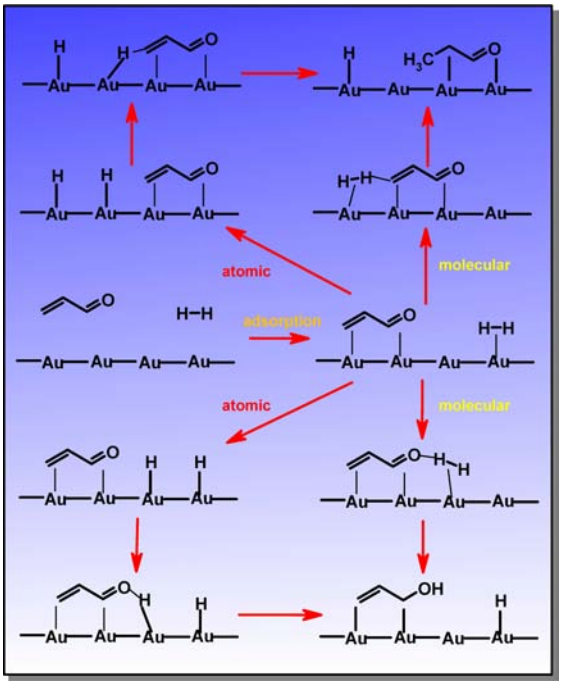

[a]The initial state is defined as the gaseous $C_3H_4O + H_2$ and the surface slab.

2. COMPUTATIONAL DETAILS

DFT calculations were carried out with periodic slab models using VASP code.[19−22] The generalized gradient approximation was used with the Perdew−Wang 91 exchange-correlation functional.[23] The interaction between atomic cores and electrons were described with the projector augmented wave method.[24,25] The same computational parameter settings have been utilized in the literature and are proven to be sufficient to describe similar systems.[26−32] Five gold surfaces exposing gold atoms with different coordination numbers were systematically considered, which, for the purposes of this study, are denoted as Au(111), Au(211), Au(211)-defect, Au(111)-mono, and Au(111)-mono-defect with decreasing Au coordination numbers, and the corresponding structures are represented in Figure 1. Four-layer slabs and 4×4 surface super cells were used for the (111)-based surfaces of Au. The Au(111)-mono was generated by adding mono row of gold atoms on the surface of Au(111). The Au(111)-mono-defect was generated by removing one gold atom from the mono row gold in one super cell. Twelve-layer slabs and 2×1 surface super cells were used for the (211)-based surfaces of Au and other metals investigated in the current work. The Au(211)-defect was generated by removing one gold atom from the step edge site of Au(211). The adsorption was modeled on the top of the slabs only, and the bottom two and six layers were fixed during optimizations of Au(111)- and Au(211)-based surfaces, respectively. A vacuum of more than 12 Å was utilized in order to minimize the interaction between slabs. Respectively 2×2×1 and 4×2×1 k-point grids were used in the calculations of (111)- and (211)-based surfaces investigated. We used an energy cutoff of 500 eV, and the force threshold in structural optimization and transition state (TS) location was set to 0.05 eV/Å.

The TSs were located with a constrained minimization method, in which the distance between two reacting atoms is set at a pre-selected value, while the geometry with respect to the remaining degrees of freedom is being optimized. Therefore, one can monitor the energy along the reaction coordinate by varying the constrained distance.[33−35] The adsorption or binding energies were defined as follows:

$$E_{ad} = E_{total} - (E_g + E_{slab}) \quad (1)$$

where E_{total} is the total energy of the adsorption system, E_g is the energy of the adsorbed molecule in the gas phase, and E_{slab} is the energy of the clean slab.

3. RESULTS AND DISCUSSION

We first calculated the reaction barriers of hydrogen dissociation and the reactions of atomic and molecular hydrogen with the terminal oxygen and carbon in acrolein at different Au surfaces. The barriers are listed in Table 1, and the corresponding structures of the hydrogenation TSs are represented in Figure 2. From Table 1, two extraordinary trends can be noticed:

(1) For the terminal O, the barriers of hydrogenation by molecular hydrogen are always lower than those of H_2 dissociation and/or hydrogenation by atomic hydrogen on almost all the considered surfaces. This strongly indicates that a non-Horiuti−Polanyi hydrogenation pathway may be favored over Au catalysts.

(2) For the Horiuti-Polanyi hydrogenation pathways, though the barrier of the H_2 dissociation declines with the decrease of Au coordination number from Au(111) to Au(111)-mono-defect, the barrier of the hydrogenation by atomic H actually increases. This can be understood from the increasing adsorption strength of atomic hydrogen from Au(111) to Au(111)-mono-defect (see Table 1). In addition, for the non-

dx.doi.org/10.1021/ja408314k | J. Am. Chem. Soc. 2013, 135, 15244−15250

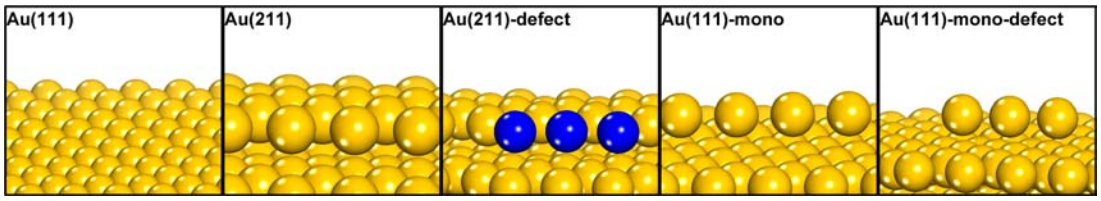

Figure 1. Structures of Au(111), Au(211), Au(211)-defect, Au(111)-mono, and Au(111)-mono-defect surfaces. Low-coordinated Au atoms on the Au(211)-defect surface are shown in dark blue.

Table 1. Calculated Barriers (eV) of Hydrogen Dissociation ($E_{a,D}$), Hydrogenation by Atomic Hydrogen ($E_{a,A}$), and Hydrogenation by Molecular Hydrogen ($E_{a,M}$) on the Terminal Oxygen and Carbon Atoms in Acrolein at Different Au Surfaces[a]

			O		C	
	$E_{a,D}$	$E_{ad,H}$	$E_{a,A}$	$E_{a,M}$	$E_{a,A}$	$E_{a,M}$
Au(111)	0.78	0.12	0.33	0.51	0.62	0.59
Au(211)	0.59	0.03	0.51	0.38	0.67	0.45
Au(211)-defect	0.67	0.07	0.58	0.32	0.67	0.70
Au(111)-mono	0.39	−0.20	0.64	0.23	0.75	0.60
Au(111)-mono-defect	0.31	−0.15	0.67	0.26	0.77	1.05

[a]The adsorption energies of hydrogen ($E_{ad,H}$) with respect to the energy of $^1/_2\,H_2$ in the gas phase on these surfaces are also listed.

Horiuti-Polanyi hydrogenation pathway, the hydrogenation barrier on terminal O falls significantly with the decrease of coordination number. Therefore, it can be generally expected that, compared to the Horiuti-Polanyi hydrogenation pathway, the non-Horiuti-Polanyi for terminal O benefits more from the low-coordination Au surfaces.

Besides the H_2 dissociation and hydrogenation on the terminal O and C atoms in acrolein, the further hydrogenation of adsorbed C_3H_5O at these gold surfaces to produce unsaturated alcohol and saturated aldehyde, which are two typical products of acrolein-selective hydrogenation, was also calculated in this work. It is clear from the barriers of all the reactions listed in Table 2 that, at Au(111), the barrier of the

Table 2. Hydrogenation Barriers (eV) by Atomic and Molecular Hydrogen on C_3H_4OH and C_3H_5O at Different Au Surfaces[a]

	$C_3H_4OH \rightarrow C_2H_3CH_2OH$		$C_3H_5O \rightarrow C_2H_5CHO$	
	$E_{a,A}$	$E_{a,M}$	$E_{a,A}$	$E_{a,M}$
Au(111)	0.50	0.72	0.82	0.55
Au(211)	0.78	1.12	0.85	1.25
Au(211)-defect	0.79	0.98	0.79	1.19
Au(111)-mono	0.51	0.80	0.90	1.15
Au(111)-mono-defect	0.57	0.70	0.45	1.14

[a]The energies of $C_3H_5O(ad)$/slab + $H_2(g)$ are set to zero to obtain the reaction barriers.

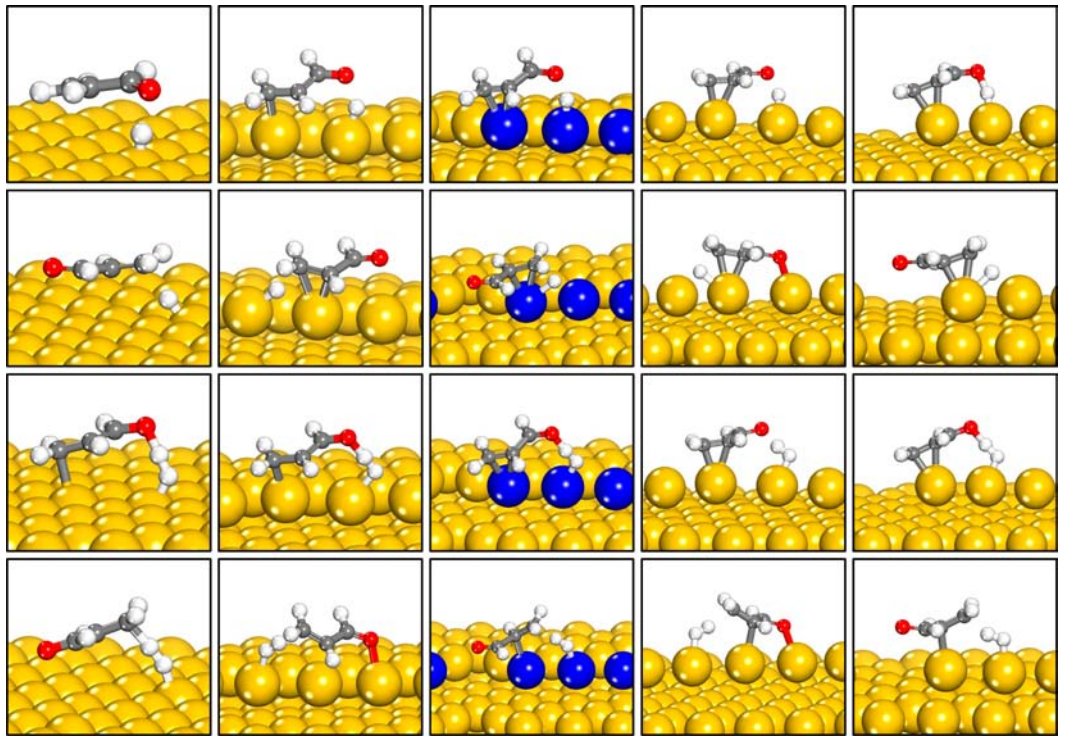

Figure 2. Transition states of the hydrogenation of the terminal O and C atoms in acrolein by atomic hydrogen (first and second panels, respectively) and the hydrogenation by molecular hydrogen (third and fourth panels, respectively) on Au(111), Au(211), Au(211)-defect, Au(111)-mono, and Au(111)-mono-defect surfaces (from left to right).

dx.doi.org/10.1021/ja408314k | J. Am. Chem. Soc. 2013, 135, 15244−15250

hydrogenation of C_3H_5O by molecular hydrogen is also lower than the corresponding Horiuti-Polanyi hydrogenation barrier, indicating again that the non-Horiuti−Polanyi mechanism may exist. The calculated structures of TSs are shown in Figure S1 in the Supporting Information.

Then, we quantitatively compared the effective barriers of both Horiuti−Polanyi and non-Horiuti−Polanyi hydrogenation pathways to firmly verify whether the non-Horiuti−Polanyi mechanism is indeed favored or not, since it is not sufficient to determine the relative preference of two different reaction pathways only by comparing the barriers of their respective elementary steps.[6,8,14,36−40] In the current work, it is found that the effective barrier is determined by the parameter $E_{TS\text{-}gas}$, which is defined as the energy of the rate-determining TS in each pathway with respect to that of the gaseous reacting species: The effective barrier can be calculated from the difference between $E_{TS\text{-}gas}$ and $E_{entropy,AC+H_2}$ (the initial state energy, defined in the caption of Figure 3). Since $E_{entropy,AC+H_2}$ is

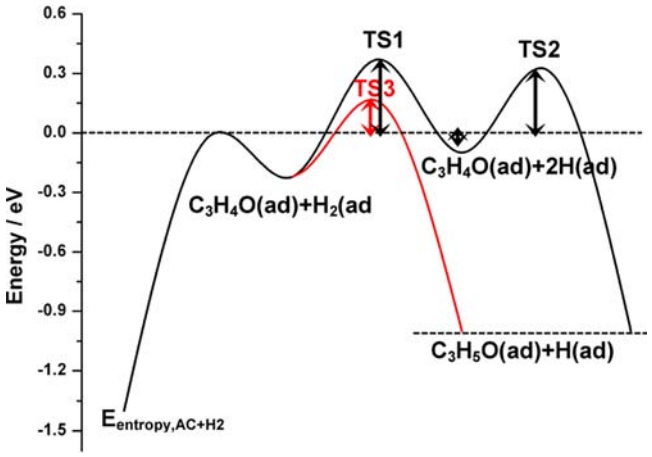

Figure 3. Energy profiles of the hydrogenation pathways of the terminal oxygen in acrolein by atomic (black line) and molecular (red line) hydrogen on Au(211). TS1, TS2, and TS3 are the transition states of hydrogen dissociation, hydrogenation by atomic hydrogen, and hydrogenation by molecular hydrogen, respectively. The gas-phase total energy of acrolein + H_2 + slab is set to zero. $E_{entropy,AC+H_2}$ is the energy with the corrections of the entropies of acrolein and hydrogen at the reaction temperature (400 K).

constant under a given reaction condition, the preference of different reaction pathways can be obtained by comparing $E_{TS\text{-}gas}$. The details of the definition and the derivation of this parameter can be found in the Supporting Information, and an example is illustrated in Figure 3 showing the energy profile of the hydrogenation of the terminal O in acrolein on Au(211), in which the energies of TS1 and TS3 are $E_{TS\text{-}gas}$ for the Horiuti−Polanyi and non-Horiuti−Polanyi hydrogenation pathways, respectively. It is clear from Figure 3 that the effective barrier of the non-Horiuti−Polanyi hydrogenation pathway is indeed lower than that of the Horiuti−Polanyi pathway for the hydrogenation of acrolein.

We further performed analyses on the factors affecting $E_{TS\text{-}gas}$. In Figure 4, two striking features discovered are illustrated. First, the $E_{TS\text{-}gas}$ values of the Horiuti−Polanyi and non-Horiuti−Polanyi hydrogenation pathways on the terminal C and O are largely linearly correlated with the coordination number of the surface-active Au atoms (Figure 4a); i.e., the value of $E_{TS\text{-}gas}$ decreases linearly with the Au coordination

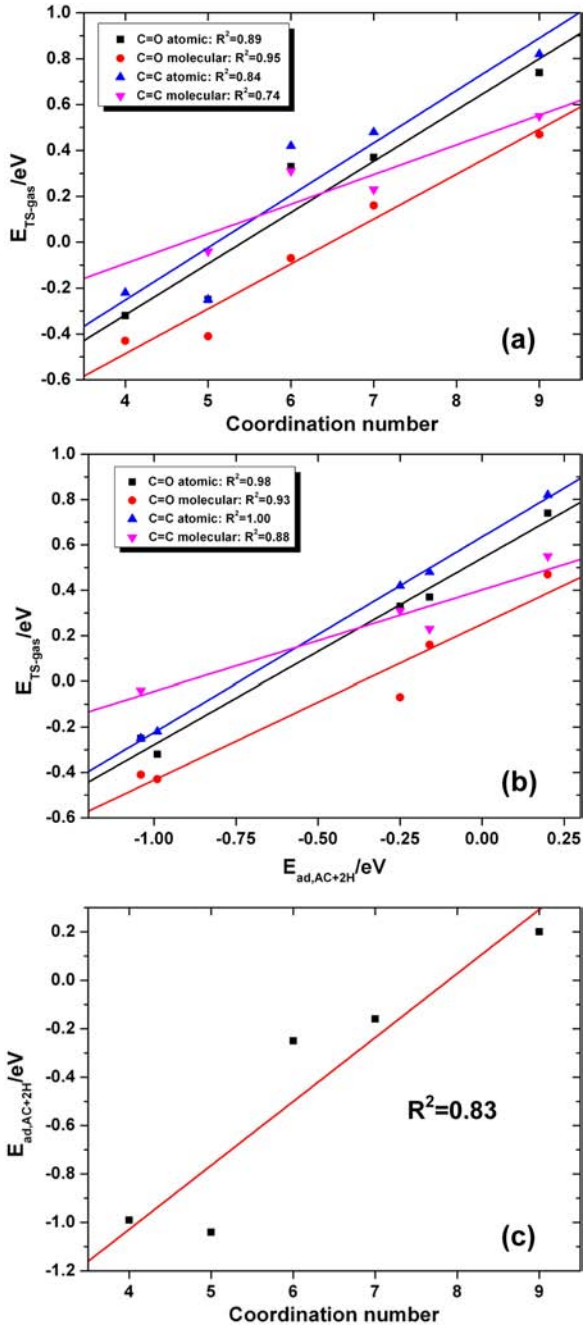

Figure 4. (a) Relationships between the energies of the transition states of the rate-determining steps with respect to the gas-phaes C_3H_4O + H_2 energy in each pathway ($E_{TS\text{-}gas}$) and the coordination numbers of the surface Au atoms. The red and blue curves are obtained from the hydrogenation reactions by molecular hydrogen on the terminal O and C of acrolein, respectively. The black and pink curves are obtained from the hydrogenation reactions by atomic hydrogen on the terminal O and C of acrolein, respectively. The energetics obtained for the hydrogenation of terminal carbon over Au(111)-mono-defect are not shown here due to the dramatically changed TS structure. (b) Correlation between the $E_{TS\text{-}gas}$ and the adsorption energy of C_3H_4O + 2H on different surfaces. (c) Correlation between the adsorption energy of C_3H_4O + 2H and the coordination number of the reactive gold atoms on different surfaces.

numbers. In fact, these observed trends between $E_{TS\text{-}gas}$ and the Au coordination numbers could be attributed to the linear relationship between $E_{TS\text{-}gas}$ and $E_{ad,AC+2H}$, which is the co-

dx.doi.org/10.1021/ja408314k | J. Am. Chem. Soc. 2013, 135, 15244−15250

adsorption energy of acrolein and two hydrogen atoms on the surfaces (Figure 4b), considering the intrinsic linear relationship between $E_{ad,AC+2H}$ and the Au coordination number (Figure 4c). These observations can be understood from the *d* band shift of these gold atoms with the variation of coordination numbers.[41,42] Second, it is interesting to note that $E_{TS\text{-}gas}$ values of the non-Horiuti−Polanyi hydrogenation pathway on the terminal O (the red curve in Figure 4a) are always lower than those of the Horiuti−Polanyi hydrogenation pathway (the black curve) regardless of the change of the coordination numbers, while for the hydrogenation on terminal C, the non-Horiuti−Polanyi hydrogenation pathway (the pink curve) will be favored once the Au coordination number of the surface atoms increases above 5 (Figure 4a). These results shed light on the fact that both surface coordination number and the hydrogenated moiety could be important for the competition between the non-Horiuti−Polanyi and the Horiuti−Polanyi schemes.

Inspired by the above results on gold surfaces, we then continued to explore the general trends in the hydrogenation reactions on the gold surfaces with regards to the Horiuti−Polanyi and non-Horiuti−Polanyi mechanisms, aiming to elucidate whether or not the non-Horiuti−Polanyi hydrogenation pathway also become favored on group 8−10 metals and other metals of group 11 (i.e., Cu and Ag). The reaction barriers of the Horiuti−Polanyi and the non-Horiuti−Polanyi hydrogenation on the terminal O atom in acrolein were calculated on Pd(211), Pt(211), Cu(211), and Ag(211) surfaces, and $E_{TS\text{-}gas}$ of each pathway was also obtained. When the $E_{TS\text{-}gas}$ values of the Horiuti−Polanyi pathway are plotted against the corresponding adsorption energies of C_3H_4O + 2H or C_3H_5O + 2H (E_{ad}) on all these surfaces, an extended Brønsted−Evans−Polanyi (BEP) type relationship can be obtained[35,43−51] (see the black curve in Figure 5). Interestingly, $E_{TS\text{-}gas}$ of the Horiuti−Polanyi hydrogenation pathway follows a single linear relationship with E_{ad}, no matter which terminal atom in acrolein is hydrogenated or on which metal surface the hydrogenation occurs; by contrast, the $E_{TS\text{-}gas}$ values from the non-Horiuti−Polanyi hydrogenation on the O and C atoms follow separate trends. Two curves from the non-Horiuti−Polanyi pathways of the hydrogenation of terminal O and C in acrolein (the blue and red curves in Figure 5) on all the surfaces studied in this work can be achieved without cross points. At the same time, one cross point between the two curves from the non-Horiuti−Polanyi and the Horiuti−Polanyi hydrogenation pathways on the terminal O in acrolein is obtained. Similar results occur on the terminal C in acrolein as well. These linear correlations clearly suggest that the assessment of the non-Horiuti−Polanyi hydrogenation pathway versus the Horiuti−Polanyi pathway strongly depends on the chemisorption energies of the reactants: the non-Horiuti−Polanyi pathway is favored in weak adsorption regions, while the Horiuti−Polanyi pathway is preferred in strong adsorption regions. These results not only disclose the possibility of the non-Horiuti−Polanyi hydrogenation mechanism on other metals, but also provide a generalized framework to predict the dominant hydrogenation mechanism on any given catalyst. This is rather important, because the rational design of new catalysts strongly depends on the mechanistic insight into the reaction systems. For example, Nørskov and co-workers have shown that different CO oxidation mechanisms gave rise to different activity trends of catalysts.[52]

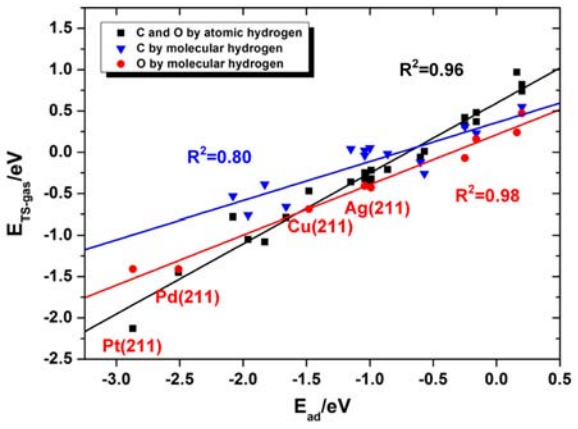

Figure 5. Relationships between the energies of the transition states of the rate-determining steps referred to the gas-phaes C_3H_4O + H_2 or C_3H_5O + H_2 energy in each pathway ($E_{TS\text{-}gas}$) and the adsorption energies of C_3H_4O + 2H or C_3H_5O + 2H (E_{ad}). $E_{TS\text{-}gas}$ is defined in the main text and the Supporting Information. The black curve is obtained from the hydrogenation reactions by atomic hydrogen, and the red and blue curves are obtained from the hydrogenation reactions by molecular hydrogen on the terminal O and C of acrolein, respectively.

In addition, from Figure 5, one may find that the hydrogenation of O is always easier than C in the non-Horiuti−Polanyi scheme on the investigated surfaces. This leads to the cross point between the curves of the non-Horiuti−Polanyi and Horiuti−Polanyi pathways of the hydrogenation of terminal O in acrolein located in higher chemisorption region compared to that of the hydrogenation on terminal C. To deeply understand these results, we adopted the energy decomposition method,[46,53] in which the barriers are decomposed into the sum of three terms, E_{AC}, E_{H_2}, and E_{int}, where E_{AC} (E_{H_2}) is the energy loss for separate reactant acrolein (H_2) to evolve from adsorption in the initial state (IS) to that in the TS, and E_{int} is the interaction energy between acrolein and H_2 at the TS.

We find that the difference between E_{AC} for hydrogenation of terminal oxygen and that of the carbon of acrolein ($E^C_{AC} - E^O_{AC}$) is linearly related to the difference between the corresponding hydrogenation barriers ($E^C_a - E^O_a$). It can also be noted in Figure 6a that the variations of ($E^C_{H_2} - E^O_{H_2}$) and ($E^C_{int} - E^O_{int}$) are smaller than that of $E^C_{AC} - E^O_{AC}$. These results suggest that the higher hydrogenation barrier of the terminal C atom than that of O may be largely due to the difference between the acrolein activation from the IS to the TS during the hydrogenation of terminal C (E^C_{AC}) and O (E^O_{AC}). We also calculated the adsorption induced charge density differences of the fully optimized acrolein in the IS adsorption and that in its fixed TS structure at Au(211) (see Figure 6b−d). The charge density difference ($\Delta\rho$) is defined as

$$\Delta\rho = \rho_{\text{acrolein/Au(211)}} - \rho_{\text{Au(211)}} - \rho_{\text{acrolein}} \quad (2)$$

where $\rho_{\text{acrolein/Au(211)}}$ is the charge density distribution of acrolein adsorbed on Au(211), and $\rho_{\text{Au(211)}}$ and ρ_{acrolein} are the charge density distributions of isolated Au(211) and acrolein, respectively. It can be clearly seen that the charge distribution of acrolein at the TS of the non-Horiuti−Polanyi hydrogenation on the terminal O atom is very similar to that in the fully optimized IS adsorption, resulting in a small E^O_{AC}, while its TS structure in non-Horiuti−Polanyi hydrogenation on the terminal carbon is apparently distorted compared with the IS,

dx.doi.org/10.1021/ja408314k | J. Am. Chem. Soc. 2013, 135, 15244−15250

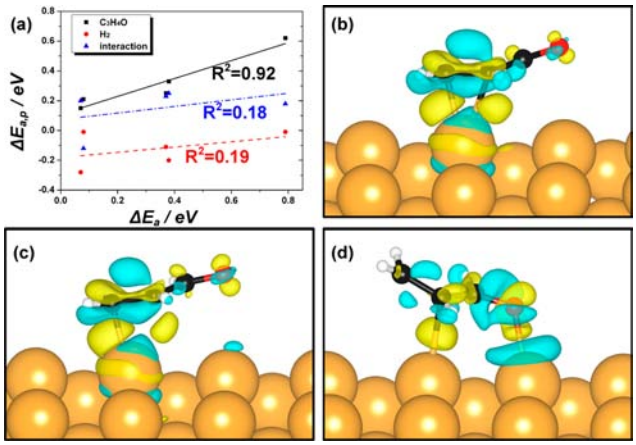

Figure 6. (a) Relationships between $\Delta E_{a,p}$ and ΔE_a. $\Delta E_{a,p}$ is calculated from $E_{AC}^{C} - E_{AC}^{O}$ (black), $E_{H_2}^{C} - E_{H_2}^{O}$ (red), and $E_{int}^{C} - E_{int}^{O}$ (blue), and $\Delta E_a = E_a^C - E_a^O$. Small R^2 values of the red and blue curves suggest very low correlations between $\Delta E_{a,p}$ and $E_{H_2}^{C} - E_{H_2}^{O}$ and $E_{int}^{C} - E_{int}^{O}$, respectively. (b–d) Electron density difference plots for the adsorption of (b) C_3H_4O on Au(211), (c) C_3H_4O at the TS of hydrogenation by molecular hydrogen on the terminal oxygen atom on Au(211), and (d) C_3H_4O at the TS of hydrogenation by molecular hydrogen on the terminal carbon atom on Au(211). The yellow contours represent charge accumulations, and the blue contours denote charge depressions. The scales of the charge densities are identical.

giving rise to a larger E_{AC}^{C}. This explanation, from the electronic point of view, may be generally vital in the understanding of the different reaction barriers observed.

The above trends clearly show when the Horiuti–Polanyi or the non-Horiuti–Polanyi mechanism is preferred for a hydrogenation reaction, and may also help us to reveal the origin of their preference. An intuitive answer is simply that, on inert metals, the H_2 dissociation is too difficult and the hydrogenation by molecular hydrogen appears to be the only way to achieve the reaction. As shown in Figure 5, the extended (linear) BEP relationships from the non-Horiuti–Polanyi and the Horiuti–Polanyi hydrogenations exhibit different slopes, which inevitably leads to the cross points. As a consequence, the non-Horiuti–Polanyi hydrogenation is favorable in some regions and unfavorable in others. Then, quantitatively speaking, the origin of the different slopes of these curves will be crucial to the understanding of the preference toward each different mechanism. It has been suggested in the literature that the slope of a classical BEP curve is related to the early or late nature of the TS.[51] Therefore, we analyzed the extended BEP relationships obtained in the current work and the classic examples in the literature (see Supporting Information for details). It was found that an early TS will give rise to an extended BEP curve with a slope close to 1. The slopes of the extended BEP curves from the hydrogenation of terminal O by atomic and molecular hydrogen and from the hydrogenation of terminal C by molecular H_2 (Figure 5) are 0.85, 0.60, and 0.47, respectively. This is then due to the fact that the TS structures of the hydrogenation by atomic hydrogen and hydrogenation of the O atom by molecular hydrogen are more similar to the corresponding initial state structures than those of the hydrogenation by molecular hydrogen on the C atom, as can be seen from the TS structures shown in the Supporting Information.

4. CONCLUSIONS

In summary, we have examined the universality of the Horiuti–Polanyi mechanism, a widely accepted mechanism proposed almost a hundred years ago, in several hydrogenation systems over different catalysts. The prevalence of the non-Horiuti–Polanyi mechanism over the Horiuti–Polanyi mechanism on a series of metals has been systematically investigated for the first time, and the effective barriers for the respective reactions have been found to be useful in distinguishing between the two mechanisms. In particular, for the hydrogenation of acrolein at different surfaces, linear relationships with different slopes were determined between the effective barriers of the hydrogenation reactions via different mechanisms and the adsorption energies of 2H + substrate. Accordingly, the relative slopes of different linear curves may determine the cross point positions, namely the preference toward the non-Horiuti–Polanyi or Horiuti–Polanyi mechanism: In the weak adsorption regions, the non-Horiuti–Polanyi mechanism is favored, while the Horiuti–Polanyi mechanism dominates in the strong adsorption regions. The physical origin of the existence of the non-Horiuti–Polanyi mechanism has also been analyzed and discussed from geometric and electronic points of view. The trends obtained in this work may be of general importance to the understanding of other systems in heterogeneous catalysis, and they may have some significant implications for the design of new catalysts in the future.

■ ASSOCIATED CONTENT

Supporting Information

Derivation of $E_{TS\text{-}gas}$, BEP analyses, and tables of adsorption and binding energies, $E_{TS\text{-}gas}$ values, and bond distances in the TSs. This material is available free of charge via the Internet at http://pubs.acs.org.

■ AUTHOR INFORMATION

Corresponding Authors

xmcao@ecust.edu.cn
p.hu@qub.ac.uk

Notes

The authors declare no competing financial interest.

■ ACKNOWLEDGMENTS

This work is financially supported by National Key Basic Research Program of China (2013CB933201, 2010CB732300, and 2011CB808505), National Natural Science Foundation of China (21073060, 21333003 and 21303051), and "111" program (B08021). Computing time in the National Super Computing Center in Jinan is acknowledged.

■ REFERENCES

(1) Gallezot, P.; Richard, D. *Catal. Rev.-Sci. Eng.* **1998**, *40*, 81.
(2) Borodziński, A.; Bond, G. C. *Catal. Rev.-Sci. Eng.* **2006**, *48*, 91.
(3) Borodziński, A.; Bond, G. C. *Catal. Rev.-Sci. Eng.* **2008**, *50*, 379.
(4) Loffreda, D.; Delbecq, F.; Vigné, F.; Sautet, P. *Angew. Chem., Int. Ed.* **2005**, *44*, 5279.
(5) Lim, K. H.; Mohammad, A. B.; Yudanov, I. V.; Neyman, K. M.; Bron, M.; Claus, P.; Rösch, N. *J. Phys. Chem. C* **2009**, *113*, 13231.
(6) Yang, B.; Wang, D.; Gong, X.-Q.; Hu, P. *Phys. Chem. Chem. Phys.* **2011**, *13*, 21146.
(7) Ide, M. S.; Hao, B.; Neurock, M.; Davis, R. J. *ACS Catal.* **2012**, *2*, 671.

(8) Manyar, H. G.; Yang, B.; Daly, H.; Moor, H.; McMonagle, S.; Tao, Y.; Yadav, G. D.; Goguet, A.; Hu, P.; Hardacre, C. *ChemCatChem* **2013**, *5*, 506.
(9) Horiuti, J.; Polanyi, M. *Nature* **1933**, *132*, 819.
(10) Horiuti, J.; Polanyi, M. *Nature* **1933**, *132*, 931.
(11) Horiuti, J.; Polanyi, M. *Nature* **1934**, *134*, 377.
(12) Horiuti, J.; Polanyi, M. *Trans. Faraday Soc.* **1934**, *163*, 1164.
(13) Naito, S.; Tanimoto, M. *J. Chem. Soc., Chem. Commun.* **1988**, 832.
(14) Yang, B.; Cao, X.-M.; Gong, X.-Q.; Hu, P. *Phys. Chem. Chem. Phys.* **2012**, *14*, 3741.
(15) Bridier, B.; López, N.; Pérez-Ramírez, J. *J. Catal.* **2010**, *269*, 80.
(16) Claus, P.; Bruckner, A.; Mohr, C.; Hofmeister, H. *J. Am. Chem. Soc.* **2000**, *122*, 11430.
(17) Mohr, C.; Hofmeister, H.; Radnik, J.; Claus, P. *J. Am. Chem. Soc.* **2003**, *125*, 1905.
(18) Brandt, K.; Chiu, M. E.; Watson, D. J.; Tikhov, M. S.; Lambert, R. M. *J. Am. Chem. Soc.* **2009**, *131*, 17286.
(19) Kresse, G.; Hafner, J. *Phys. Rev. B* **1993**, *47*, 558.
(20) Kresse, G.; Hafner, J. *Phys. Rev. B* **1994**, *49*, 14251.
(21) Kresse, G.; Furthmuller, J. *Comput. Mater. Sci.* **1996**, *6*, 15.
(22) Kresse, G.; Furthmuller, J. *Phys. Rev. B* **1996**, *54*, 11169.
(23) Perdew, J. P.; Wang, Y. *Phys. Rev. B* **1992**, *45*, 13244.
(24) Blöchl, P. E. *Phys. Rev. B* **1994**, *50*, 17953.
(25) Kresse, G.; Joubert, D. *Phys. Rev. B* **1999**, *59*, 1758.
(26) Loffreda, D.; Delbecq, F.; Vigne, F.; Sautet, P. *J. Am. Chem. Soc.* **2006**, *128*, 1316.
(27) Boronat, M.; Concepción, P.; Corma, A.; González, S.; Illas, F.; Serna, P. *J. Am. Chem. Soc.* **2007**, *129*, 16230.
(28) Gao, W.; Baker, T. A.; Zhou, L.; Pinnaduwage, D. S.; Kaxiras, E.; Friend, C. M. *J. Am. Chem. Soc.* **2008**, *130*, 3560.
(29) Rodríguez, J. A.; Feria, L.; Jirsak, T.; Takahashi, Y.; Nakamura, K.; Illas, F. *J. Am. Chem. Soc.* **2010**, *132*, 3177.
(30) Alves, L.; Ballesteros, B.; Boronat, M.; Cabrero-Antonino, J. R.; Concepción, P.; Corma, A.; Correa-Duarte, M. A.; Mendoza, E. *J. Am. Chem. Soc.* **2011**, *133*, 10251.
(31) Green, I. X.; Tang, W.; McEntee, M.; Neurock, M.; Yates, J. T. *J. Am. Chem. Soc.* **2012**, *134*, 12717.
(32) Pan, M.; Ham, H. C.; Yu, W.-Y.; Hwang, G. S.; Mullins, C. B. *J. Am. Chem. Soc.* **2013**, *135*, 436.
(33) Alavi, A.; Hu, P.; Deutsch, T.; Silvestrelli, P. L.; Hutter, J. *Phys. Rev. Lett.* **1998**, *80*, 3650.
(34) Liu, Z. P.; Hu, P. *J. Am. Chem. Soc.* **2003**, *125*, 1958.
(35) Michaelides, A.; Liu, Z. P.; Zhang, C. J.; Alavi, A.; King, D. A.; Hu, P. *J. Am. Chem. Soc.* **2003**, *125*, 3704.
(36) Yang, B.; Burch, R.; Hardacre, C.; Headdock, G.; Hu, P. *ACS Catal.* **2012**, *2*, 1027.
(37) Yang, B.; Burch, R.; Hardacre, C.; Headdock, G.; Hu, P. *J. Catal.* **2013**, *305*, 264.
(38) Nørskov, J. K.; Bligaard, T.; Kleis, J. *Science* **2009**, *324*, 1655.
(39) Meskine, H.; Matera, S.; Scheffler, M.; Reuter, K.; Metiu, H. *Surf. Sci.* **2009**, *603*, 1724.
(40) Manyar, H. G.; Morgan, R.; Morgan, K.; Yang, B.; Hu, P.; Szlachetko, J.; Sa, J.; Hardacre, C. *Catal. Sci. Technol.* **2013**, *3*, 1497.
(41) Hammer, B.; Nørskov, J. K. *Adv. Catal.* **2000**, *45*, 71.
(42) Liu, Z. P.; Hu, P.; Alavi, A. *J. Am. Chem. Soc.* **2002**, *124*, 14770.
(43) Brønsted, J. N. *Chem. Rev.* **1928**, *5*, 231.
(44) Evans, M. G.; Polanyi, M. *Trans. Faraday Soc.* **1938**, *34*, 11.
(45) Pallassana, V.; Neurock, M. *J. Catal.* **2000**, *191*, 301.
(46) Liu, Z. P.; Hu, P. *J. Chem. Phys.* **2001**, *114*, 8244.
(47) Logadottir, A.; Rod, T. H.; Nørskov, J. K.; Hammer, B.; Dahl, S.; Jacobsen, C. J. H. *J. Catal.* **2001**, *197*, 229.
(48) Nørskov, J. K.; Bligaard, T.; Logadottir, A.; Bahn, S.; Hansen, L. B.; Bollinger, M.; Bengaard, H.; Hammer, B.; Sljivancanin, Z.; Mavrikakis, M.; Xu, Y.; Dahl, S.; Jacobsen, C. J. H. *J. Catal.* **2002**, *209*, 275.
(49) Bligaard, T.; Nørskov, J. K.; Dahl, S.; Matthiesen, J.; Christensen, C. H.; Sehested, J. *J. Catal.* **2004**, *224*, 206.
(50) Loffreda, D.; Delbecq, F.; Vigné, F.; Sautet, P. *Angew. Chem., Int. Ed.* **2009**, *48*, 8978.
(51) van Santen, R. A.; Neurock, M.; Shetty, S. G. *Chem. Rev.* **2010**, *110*, 2005.
(52) Falsig, H.; Hvolbaek, B.; Kristensen, I. S.; Jiang, T.; Bligaard, T.; Christensen, C. H.; Nørskov, J. K. *Angew. Chem., Int. Ed.* **2008**, *47*, 4835.
(53) Liu, Z. P.; Hu, P. *J. Chem. Phys.* **2001**, *115*, 4977.